

Generation and Manipulation of Hierarchical Morphology in Interpenetrating Polymer Networks by Using Photochemical Reactions

Hideyuki Nakanishi, Masahiro Satoh,
Tomohisa Norisuye, and Qui Tran-Cong-Miyata*

Department of Polymer Science and Engineering,
Kyoto Institute of Technology, Matsugasaki, Sakyo-ku,
Kyoto 606-8585, Japan

Received July 3, 2004

Revised Manuscript Received October 5, 2004

Interpenetrating polymer networks (IPNs) belong to a class of molecular composites that consisted of two different networks mutually entangled by cross-link during the polymerization process. In the past decades, a large number of IPNs have been synthesized by using various techniques with the expectation that superior mechanical properties may emerge from their unique networking structures.¹ However, except for some limited cases,² phase separation occurs when the yields of polymerization or cross-link density reach a threshold. Nevertheless, these two-phase materials have found their wide applications in specialty materials such as those with high impact strength, sound, or vibration damping or with controllability of gas transport.³ Since the physical properties of IPNs strongly depend on morphology, it would be very useful to develop a convenient method to generate and control their phase-separated structures.

From the viewpoint of pattern formation process, IPN is a chemical system driven by two competing antagonistic interactions: cross-linking reactions vs phase separation. This competition is controlled by the so-called *activator–inhibitor principle*⁴ where phase separation corresponds to an activator and cross-linking reaction plays the role of an inhibitor. It has been shown that such the competition process can result in a wide variety of morphologies.⁵ Morphology control of IPNs using thermally activated reactions is generally limited because the heat used to induce chemical reactions also affects the miscibility of the mixture. As a consequence, some alternative methods are expected to efficiently manipulate the competition between phase separation and the chemical reaction. In this study, we demonstrate that photochemical reactions can provide a tool to generate and control hierarchical morphologies of IPNs in the micrometer ranges.

We have utilized photo-cross-linking reactions to freeze the spinodal structure developing in polymer blends undergoing phase separation.⁶ Though the co-continuous morphology could be generated and controlled by this particular method, the development of the characteristic length scales in these experiments was quite limited because of the drastic increase in viscosity associated with the cross-linking reaction in the bulk state of polymer. Here, to remove this constraint on the morphological length scales, we performed experiments using an IPN system containing a photo-cross-linkable polymer dissolved in a photopolymerizable monomer of the second polymer. The rates of the

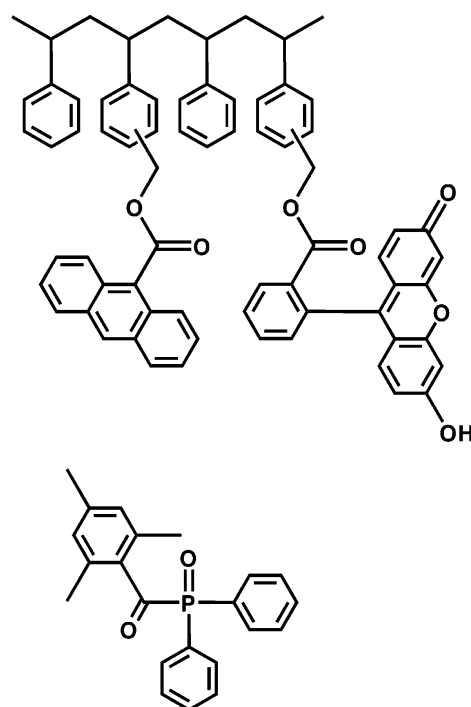


Figure 1. Upper: chemical structure of the polystyrene derivative PSAF doubly labeled with anthracene as a cross-linker and fluorescein as a marker. Lower: the photoinitiator Lucirine TPO.

cross-linking reactions as well as the photopolymerization were controlled by varying the light intensity. Furthermore, the mobility of polymer in the reacting mixture was regulated by changing the polymer molecular weight using different concentrations of photoinitiator. We show below that by simply changing the light intensity and/or the concentration of photoinitiator a variety of morphologies with different length scales as well as structural hierarchies can be generated and manipulated by irradiation.

Samples used in this work are mixtures of methyl methacrylate (MMA) monomers and polystyrene doubly labeled with anthracene and fluorescein (PSAF, $M_w = 270\,000$; $M_w/M_n = 2.4$). PSAF was synthesized by reacting a random copolymer of styrene and chloromethylstyrene (12% in mole fraction) with potassium salt of 9-anthracenecarboxylic acid (Sigma-Aldrich, recrystallized twice in methanol) in anhydrous dimethylformamide at 65 °C over 3 h.⁶ Subsequently, a dimethylformamide solution of fluorescein monosodium salt (Wako Pure Chemical Industries, Japan) was further added to the reacting solution, and the mixture was allowed to react over an additional 3 h to achieve the double labeling. The average label content of the resulting polymer is 85 anthracene moieties per chain (ca. 3.1% in mole fraction) as determined by UV spectroscopy. Under this reaction condition, only a trace of the marker fluorescein was covalently attached to the chloromethylstyrene repeat units of the copolymer. The chemical structure of PSAF is illustrated in Figure 1. Upon irradiation with 365 nm ultraviolet (UV) light, anthracene undergoes photodimerization, resulting in the PSAF networks. Furthermore, under excitation with 488 nm, fluorescence of the fluorescein marker provides

* To whom correspondence should be addressed.

a strong contrast for the PSAF-rich domains under a microscope. The precursor homogeneous solution for the IPN preparation was prepared by dissolving PSAF in distilled methyl methacrylate monomer (MMA, Wako Pure Chemical Industries, Japan) containing 2,4,6-trimethylbenzoyldiphenylphosphine oxide (Lucirin TPO, BASF, Figure 1) used as initiator for photopolymerization of MMA and ethylene glycol dimethacrylate (EGDMA, Sigma-Aldrich) as a cross-linker for PMMA chains. The precursor solution was sandwiched between the two coverslips with a 25 μm aluminum spacer used to adjust the sample thickness. The polymer solution was irradiated under a nitrogen atmosphere at ambient temperature (30 $^{\circ}\text{C}$) by using the 365 nm line of a high-pressure Hg–Xe lamp (350 W, Moritex, Japan) equipped with an optical fiber. Under this irradiation condition, the PSAF as well as PMMA networks are simultaneously generated, resulting in a *full*-IPN of polystyrene and poly(methyl methacrylate). The composition of PSAF and MMA monomer was fixed at PSAF/MMA (5/95). On the other hand, the concentration of Lucirin TPO was kept at 2 and 10 wt % with respect to the composition of MMA while the concentration of the cross-linker EGDMA was fixed at 2 wt %. Because the molar extinction coefficient of anthracene at 365 nm ($\epsilon_{365\text{nm}} = 10\,000$) is much higher than Lucirin TPO ($\epsilon_{365\text{nm}} = 450$), the PSAF component was gelled first, and its network composition is higher than PMMA. The resulting morphology was observed by using a laser scanning confocal microscope (Pascal LSM5, Carl Zeiss) equipped with an Ar^+ ion laser (488 nm) used to excite the fluorescein marker on the PSAF component. Morphology of the resulting IPNs was observed with an objective lens ($\times 20$, N.A. = 0.5) for low magnification and with an oil-immersed objective lens ($\times 63$, N.A. = 1.4) for high magnification. The optical micrographs were taken with the dimensions (512 pixels \times 512 pixels) and the resolution 0.7 μm in the z -direction. The images were taken at 0.3 μm depth intervals, from which the 3-dimensional images were constructed by using the software Image Visart (v. 2.08, Carl Zeiss). Further analysis such as particle size distribution was performed with conventional image analysis software (ImageHyper II, Digimo Inc., Japan).

Illustrated in Figure 2 is the typical morphology resulting from the competition process between phase separation and the networking reactions of PSAF and PMMA. The cross-linking densities and the molecular weight between cross-link junctions of PMMA were varied by changing the light intensity and the photoinitiator concentration. For a given light intensity, increasing concentration of Lucirin TPO results not only in a hierarchical morphology but also in a phase inversion. An example is illustrated in Figure 2(A1,B1). Here the light intensity was 0.01 mW/cm^2 , and the concentration of Lucirin TPO was kept at 2 and 10 wt % with respect to MMA. Irradiation time was fixed at 60 min throughout the experiments. Shown in these figures are the confocal images of the morphology taken in the x – y plane (460.6 $\mu\text{m} \times 460.6 \mu\text{m}$) at the depth located at $z = 5 \mu\text{m}$ from the surface of a 25 μm thick samples. The bright fluorescent regions in the images correspond to the PSAF-rich region, whereas the dark nonfluorescent domains are rich in PMMA. Obviously, an increase from 2 to 10 wt % in the photoinitiator concentration results in a phase inversion. The domains obtained with higher concentration of Lucirin TPO (10 wt %) are more regulated compared to the case of low

initiator concentration (2 wt %). The spherical domain sizes distribution in these two morphologies was measured by image analysis techniques, and the results are shown in Figure 2(A2,B2). The width σ of the distribution was quantitatively evaluated by fitting the experimental results to the following modified Gaussian function:

$$N(\xi) = A \exp[-(\xi - \xi_0)^2/\sigma^2] \quad (1)$$

Here ξ and ξ_0 are respectively the diameter of the droplets and their mean value. σ is the width of their distribution, and A is the number of droplets with the diameter ξ_0 . For both cases of irradiation, it was found that though the average length scale ξ_0 of the droplets is almost the same, ca. 40 μm , the size distribution is broader for the case using 2 wt % of Lucirin ($\sigma = 11.8 \mu\text{m}$) compared to 10 wt % ($\sigma = 8.2 \mu\text{m}$). Since irradiation intensity, irradiation time, and the composition of the IPN precursor solution were kept constant, the sharpening of the domain distribution in the case of higher Lucirin concentration would be caused by the decrease in the molecular weights between cross-link junctions of PMMA chains. It is worth noting that under higher magnification it was found that there exists in the PSAF-rich droplets of Figure 2B1 the secondary droplets rich in PMMA. Such a hierarchical morphology has been previously observed at much smaller length scales in the case of inhomogeneous quenching conditions such as two-step temperature jump.^{7,8} By scanning the morphology along the vertical (z) direction with a 0.3 μm interval, three-dimensional (3D) images of the IPNs obtained under these two conditions were constructed. As shown in Figure 2(A3,B3), the fluorescent images taken in the yz - and xz -planes of the IPN indicate that these PMMA-rich (dark) regions are partially interconnecting with each other. The corresponding 3D morphologies are illustrated in Figure 2(A4,B4). Obviously, not only the PSAF-rich regions are interconnected, but the PMMA-rich regions that appear as transparent in Figure 2A4 are also connected with each other. The particular structure of the PMMA-rich phase seen in Figure 2A4 probably reveals the so-called “interconnecting cylinders” which have been previously proposed in the literature⁹ with some evidence obtained by transmission electron microscopy (TEM) and small-angle neutron scattering (SANS) for poly(*cross*-styrene)-inter-poly(*cross*-butadiene) IPNs.¹⁰

The minor phases in the PSAF-rich as well as PMMA-rich regions were also observed in the 3D morphology. The 3D image of the morphology obtained with 10 wt % of Lucirin TPO is illustrated in Figure 2B4, showing that those PMMA-rich domains within the PSAF-rich phase seem to be interconnected throughout the PSAF-rich matrix. On the other hand, upon increasing light intensity to $I = 0.10 \text{ mW}/\text{cm}^2$, spinodal-like structure with the period ca. 90 μm emerged. Under higher magnification, it was found that there exists a secondary PMMA-rich phase inside these large-scale spinodal structures. The 2-D Fourier transform of the IPN morphology reveals two distinct peaks as depicted in Figure 2C2. The peak in the large q range corresponds to the interparticle distance in the secondary PMMA-rich phase within the PSAF-rich interconnecting domains, whereas the broad peak in the small q range reflects the period of the spinodal structure. The Bragg spacing calculated from $\xi = 2\pi/q_{\text{max}}$, where q_{max} is the

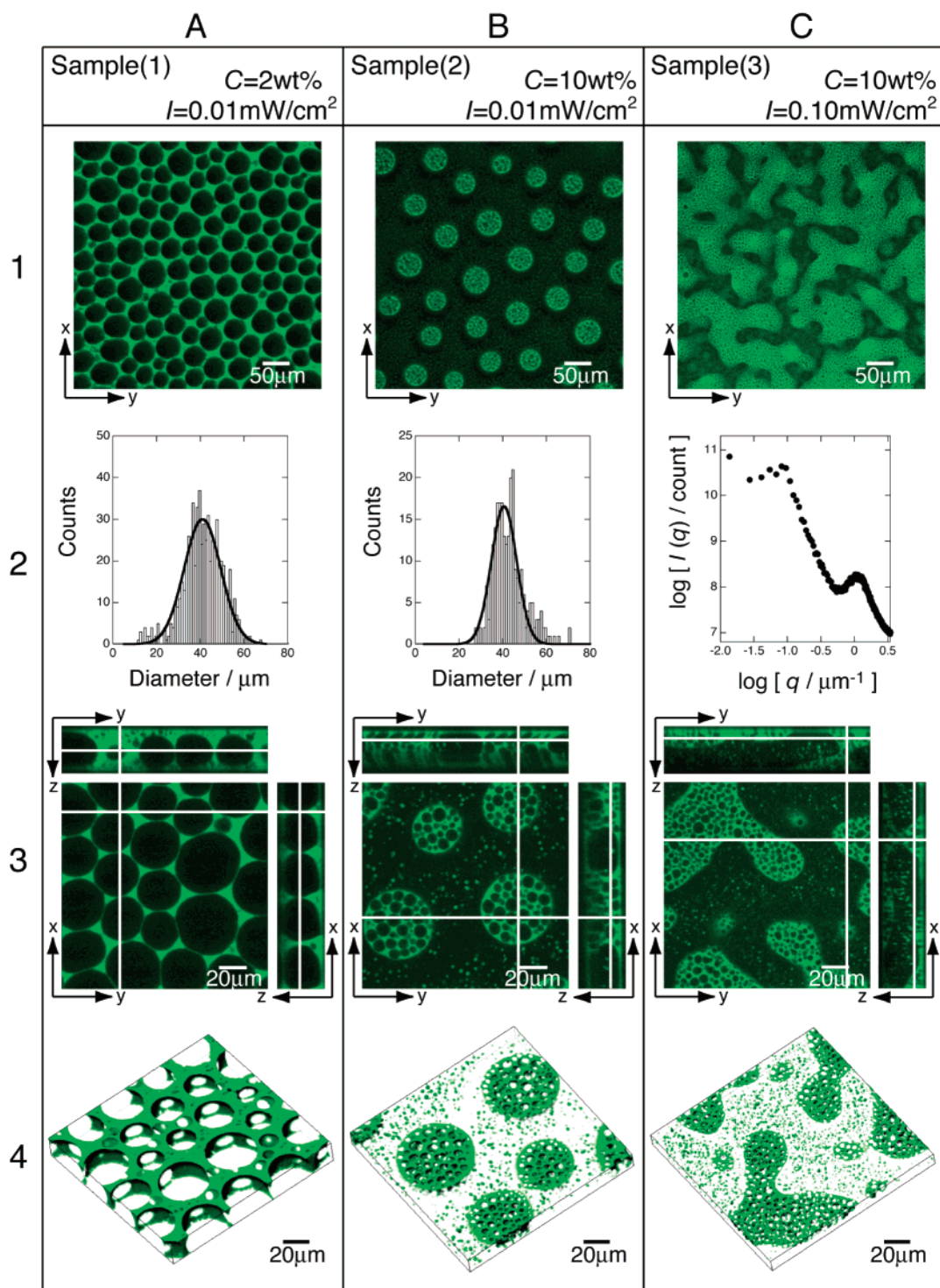


Figure 2. Morphology of the poly(*cross*-styrene)-*inter*-poly(*cross*-methyl methacrylate) IPNs obtained by varying the concentration of photoinitiator (*C*) and the light intensity (*I*) at 25 °C.

position of the broad peak in the 2D-FFT power spectra shown in Figure 2C2, coincides with the average period of the spinodal structure of the IPN. Similar morphology with multiple length scales has been reported recently for reactive blends under continuous quenching.¹¹ For comparison, the 3D morphology of sample 3 is illustrated in Figure 2C4.

We have shown that polymers with hierarchical structures can be obtained by using light to simultaneously induce photo-cross-link and photopolymerization. The nonuniform cross-linking kinetics of IPNs is a main reason for the formation of morphology with

multiple length scales.^{12,13} In general, cross-linking is a useful method to control morphology of polymer blends as well as block copolymers as recently demonstrated.¹⁴ Compared to thermally activated reactions, better control over the morphological length scales was achieved because of the quench depth can be precisely adjusted by regulating the light intensity. As a consequence, the length scale of the morphology can be brought up to hundreds of microns. From the 3-dimensional imaging using fluorescent markers, the so-called “interconnecting cylinder morphology” proposed previously by Sperling and co-workers was experimentally confirmed.

Experiments on the interplay between reaction kinetics and phase separation in IPNs over large length scale and time scale are in progress by using two different polymer networks induced independently by two different excitation wavelengths. These results will be reported later.

Acknowledgment. This work was financially supported by the Ministry of Education (MONKASHO), Japan, through the priority-research-area "Dynamic Control of Strongly Correlated Soft Materials" (No. 13031054). We thank Dr. Kazuo Ashikaga (Matsui Chemicals Inc., Kyoto) for useful discussion and generous gifts of chemicals used for photopolymerization described in this work. The kind help of Dr. Lipin Sung (National Institute of Standards and Technology (NIST)) in the beginning of this project was gratefully acknowledged.

References and Notes

- (1) *Interpenetrating Polymer Networks*; Klempner, D., Sperling, L. H., Utracki, L. A., Eds.; Advances in Chemistry Series No. 293; American Chemical Society: Washington, DC, 1994.
- (2) For example, see: Frisch, H. L.; Hua, Y. S. *Macromolecules* **1989**, *22*, 91.
- (3) *IPNs Around the World—Science and Engineering*; Kim, S. C., Sperling, L. H., Eds.; John Wiley & Sons: New York, 1997.
- (4) *Chemical Waves and Patterns*; Kapral, R., Showalter, K., Eds.; Kluwer Academic Publishers: Boston, MA, 1995.
- (5) Seul, M.; Andelman, D. *Science* **1995**, *267*, 476.
- (6) (a) Tran-Cong, Q.; Nagaki, T.; Nakagawa, T.; Yano, O.; Soen, T. *Macromolecules* **1989**, *22*, 2720. (b) Imagawa, A.; Tran-Cong, Q. *Macromolecules* **1995**, *28*, 8388. (c) Harada, A.; Tran-Cong, Q. *Macromolecules* **1997**, *30*, 1643.
- (7) Okada, M.; Fujimoto, K.; Nose, T. *Macromolecules* **1995**, *28*, 1795.
- (8) Lee, D. S.; Kim, S. C. *Macromolecules* **1984**, *17*, 268. See also Chapter 3 in ref 3.
- (9) An, J. H.; Fernandez, A. M.; Sperling, L. H. *Macromolecules* **1987**, *20*, 191.
- (10) Budford, R.; Chaplin, R.; Mai, Y. M. In *Multiphase Macromolecular Systems*; Culbertson, B. M., Ed.; Contemporary Topics in Polymer Science; Plenum: New York, 1989; Vol. 6.
- (11) Alig, I.; Rullmann, M.; Holst, M.; Xu, J. *Macromol. Symp.* **2003**, *198*, 245.
- (12) Tran-Cong, Q.; Harada, A.; Kataoka, K.; Ohta, T.; Urakawa, O. *Phys. Rev. E* **1997**, *55*, R6340.
- (13) Okada, M.; Masunaga, H.; Furukawa, H. *Macromolecules* **2000**, *33*, 7238.
- (14) Hahn, H.; Eitouni, H. B.; Balsara, N. P.; Pople, J. A. *Phys. Rev. Lett.* **2003**, *90*, 155505.

MA048657I